Title: Label-free based proteomics analysis of protein changes in frozen whiteleg shrimp (*Litopenaeus vannamei*) pre-soaked with sodium trimetaphosphate

Author names: Bin Zhang[1,*], Jun-long Mao[1], Hui Yao[1], Santiago P., Aubourg[2,*]

Affiliations: 1. Key Laboratory of Health Risk Factors for Seafood of Zhejiang Province, College of Food Science and Pharmacy, Zhejiang Ocean University; 2. Consejo Superior de Investigaciones Cientificas (CSIC), Inst Invest Marinas

Corresponding author*: Bin Zhang, Tel: +86-0580-255-4781, E-mail: zhangbin@zjou.edu.cn, or zhangbin_ouc@163.com, ORCID: 0000-0003-4696-9098; Aubourg, Santiago P., e-mail: saubourg@iim.csic.es

Corresponding address*: No.1, Haida South Road, Lincheng Changzhi, Zhoushan, Zhejiang province, 316022 P. R. China (Zhang B); Marine Research Institute (CSIC), Eduardo Cabello, 6. 36208-Vigo, Spain (Aubourg SP)

Abstract: Muscle proteins in peeled shrimp (*Litopenaeus vannamei*) are known to be unstable and prone to denaturation affected by freezing and frozen storage. In this study, label-free proteomics were performed to explore the stabilization of frozen (30 days at -18 ºC) muscle proteins when a pre-soaking treatment with distilled water (DW)- and sodium trimetaphosphate (ST) was applied; comparison to fresh samples (FS) was carried out. In total, 163 differentially abundant proteins (DAPs) were down-regulated in DW *vs*. FS, these including ribosomal proteins, actins, myosin, paramyosin, myosin heavy chains, and tropomyosin; interestingly, most of these DAPs (181 proteins) were up-regulated in ST *vs*. DW mainly due to the incorporation of ST into muscle tissues. The results revealed the decreased protein degradation resulting from the reduced damage from ice-crystal growth. Gene ontology (GO) analysis suggested that these DAPs were mainly involved in catalytic activity, binding, and metabolic processes. Kyoto encyclopedia of genes and genomes (KEGG) results indicated that many pathways, including phototransduction, metabolic, and ribosomal pathways that interacted with phosphoglycerate mutase, actins, and ribosomal proteins, were altered. Additionally, Eukaryotic clusters of orthologous group (KOG) results confirmed that incorporated ST maintained the stability of these DAPs in shrimp muscle, especially for cytoskeleton proteins, and retarded the degradation of muscle proteins during frozen storage.

Keywords: Label-free proteomics; sodium trimetaphosphate soaking; frozen storage; shrimp; protein degradation

1. Introduction

Whiteleg shrimp, *Litopenaeus vannamei*, is a very popular aquaculture species for consumers, given its great sensory characteristics and highly nutritional values. Frozen storage, as a primary processing method, can remarkably preserve the quality of shrimp products, owing to its ability of suppressing protein degradation and inhibiting microbial growth during long-term storage. However, the quality of frozen-stored shrimp product is greatly limited by the cold-induced denaturation and oxidation of myofibrillar proteins (MPs) in the muscle, due to the formation and growth of ice crystals, the dehydration of proteins, and solute concentration in the tissues (Zhang, Yao, Qi, & Ying, 2020). Notably, large ice-crystals formed gradually in frozen shrimp muscle can damage the fibers and connective tissues, thus resulting in increased drip loss and decreased nutrition value as a result of subsequent thawing and processing (Zhang, Cao, Lin, Deng, & Wu, 2019). Myofibrillar proteins, the most abundant protein group, in shrimp muscle are relatively unstable and prone to denaturation during transport and storage, as they are influenced by temperature, type of additives present, ionic strength, and storage length, which can result in deterioration and affect negatively the muscle quality (Shi, Lei, Shen, Hong, Yu, Zhu, & Luo, 2019).

In order to suppress protein denaturation in frozen shrimp muscle, several additives have been tested to ensure maximum protein functionality (Oliveira & Goncalves, 2019). Polyphosphates are legal food additives (generally regarded as

safe, GRAS) that are commonly used in processed fish and shrimp products to maintain their water-holding capacity (WHC), reduce drip loss, retard oxidative rancidity, and maintain color stability during long storage periods. Polyphosphates (polyanions) treatment enhances the electrostatic repulsion of muscle proteins and promote the pH deviation from the average isoelectric point of proteins, which allow more water molecules to be bounded or trapped within myofibrils and tissue cells, thereby reducing the fluid loss upon thawing and cooking. Consequently, polyphosphates treatment would increase the WHC of muscle, which likely contributes to protein stabilization against denaturation during freezing and frozen storage (Wachirasiri, Wanlapa, Uttapap, & Rungsardthong, 2016). Despite the findings of these previous studies, the cryoprotective mechanisms by which polyphosphates treatment affects the stability of protein (proteome) in frozen peeled shrimp still require investigation. Furthermore, little information is available on the use of proteomics to explore the cryoprotective mechanisms of polyphosphates.

Proteomics is a scientific approach of analyzing and identifying large-scale proteins based on mass spectrometry (MS). In recent years, label-free proteomics has been regarded as a promising and powerful procedure to understand the molecular connections between quality traits and muscle proteins, which enable high-throughput analysis for determining the differential expression levels of proteins in muscle. The current study was conducted to explore the cryoprotective mechanisms involved in the stabilization of muscle proteins in frozen whiteleg shrimp by sodium trimetaphosphate (TS) as a representative molecule of polyphosphates. Specifically,

the proteomic characteristics were investigated by label-free proteomics analysis. Further applications of these findings may server as a foundation for uncovering the cryoprotective mechanisms of phosphate treatments used in frozen shrimp products.

Maybe it could be eliminated here. Furthermore, the meaning is not clear.

2. Materials and methods

2.1 Chemicals

Sodium trimetaphosphate ($[Na_3(PO_3)_3]$) was obtained from Aladdin Biochemical Technology Co., Ltd. (Shanghai, China). Trypsin was purchased from Thermo Fisher Scientific Co., Ltd (Shanghai, China). A protease inhibitor cocktail (protease arrest) and a BCA assay kit were procured from Merck & Co., Inc. (MN, USA). Dithiothreitol (DTT), thiourea, acetonitrile (ACN), formic acid (FA), ammonia, iodinated acetamide (IAA), tris(hydroxymethyl)aminomethane (Tris), dithiothreitol, carbamide, and ammonium bicarbonate used in this study were supplied by Chemical Reagents Co., Ltd. (Shanghai, China).

2.2 Shrimp preparation

Live shrimp measuring 10.3–12.7 cm in length and 20.8–24.0 g in weight, were purchased from a located supermarket in Zhoushan, China. The samples were placed in a cooler filled with ice and transported to the lab within 20 min. Upon arrival, the shrimp were taken out and cleaned using cold water. Next, peeled shrimp were manually prepared by removing the head, shell, tail, and devein. The samples were sorted according to size and then (maybe this words could be avoided) randomly

111 divided into three batches, including a fresh shrimp batch (FS, without soaking), a
112 distilled water soaked-shrimp batch (DW, as negative control), and an aq. 3% (w/v)
113 $Na_3(PO_3)_3$ soaked-shrimp (ST) batch. After soaking at 0-4°C for 3 h, shrimp muscle
114 was took out and drained at 4°C for 3 min, and subsequently kept at -30°C for 3 h.
115 Then, the obtained samples were put into polystyrene boxes (20 × 15 × 5 cm) and
116 rapidly covered with polyethylene film (150 μm thickness).

117 ***2.3 Protein extraction***

118 Briefly, frozen muscle was rapidly powdered with a pestle in a pre-chilled mortar
119 containing liquid nitrogen. Next, the pulverized samples (100 ± 3 mg) were mixed
120 with 400 μL of pre-cold (0–4°C) extraction buffer (containing 100 mmol/L Tris-HCl,
121 1% (w/v) DTT, 1% (v/v) protease arrest, 2.0 mol/L thiourea, and 8.0 mol/L urea) in a
122 5-mL centrifuge tube. Next, the mixture was homogenized using a PT1200E
123 homogenizer (Kinematcia, Lucerne, Switzerland). The resulting mixture was
124 centrifuged at 10,000 × *g* for 20 min (4°C) in a Pico 17 centrifuge (Thermo Scientific,
125 Shanghai, China). Finally, the harvested supernatant was transferred to another tube
126 for the following digestion and proteomic analysis. The concentrations of extracted
127 proteins were determined by using a BCA assay kit according to the instructions.

128 ***2.4 Trypsin digestion***

129 Extracted proteins (50 μg) were reduced with 1 mol/L DTT solution at 60°C for
130 30 min, and subsequently alkylated with 1 mol/L IAA at 25°C for 30 min in a dark
131 room. Next, 100 mmol/L Tris-HCl buffer (pH 8.0) containing 8 mol/L urea were
132 added to the mixture. After centrifugation at 12,000 × *g* for 3 min (4°C), the same

Tris-HCl buffer were added to the resulting supernatant, centrifugation being carried out again under the same conditions. Subsequently, the supernatant was collected and diluted by adding 50 mmol/L NH_4HCO_3 solution, and then centrifuged at 12,000 × *g* for 3 min (4°C). Next, trypsin was added at 1:50 trypsin to protein mass ratio to digest proteins at 37°C for 16 h. The digestion incubation was terminated by the addition of 10% (v/v) FA solution. The peptide mixture solution was then desalted by using C18 ZipTip pipette tips (Millipore China Ltd., Shanghai, China). Finally, the resulting peptide solution were lyophilized and resuspended in 0.2% (v/v) FA for the HPLC-MS/MS analysis.

2.5 HPLC-MS/MS analysis

The tryptic peptides were determined by using an easy nLC/Ultimate 3000 nano-HPLC coupled on-line to an Orbitrap fusion lumos MS system (Thermo Fisher Scientific, Bremen, Germany). Briefly, samples dissolved in 0.1% FA were loaded onto a self-made reversed-phase column (75 μm × 50 cm, 3 μm). The concentrated peptides were loaded on a C_{18} analytical column (150 μm × 120 mm, 1.9 μm) at a flow rate of 450 nL/min, where a binary mobile phase was used: 0.1% (v/v) FA in water (phase A) and 0.1% (v/v) FA in acetonitrile/water (8:2, v/v) (phase B). After the gradient elution, the full-scan MS was performed using the following procedure: automatic gain control (AGC) target, 3e6; resolution, 120,000; scan range, 300−1400 *m/z*; and maximum injection time, 80 ms. The dd-MS spectra was recorded from 200 *m/z* to 2000 *m/z*, 45 ms maximum injection time, an 5e4 AGC target value, and a 15,000 resolution. The isolation window, minimum AGC target, intensity threshold,

and dynamic exclusion were set to 1.6 *m/z*, 5.00e2, 1.1e4, and 12.0 s, respectively.

2.6 Protein identification

The identification of resulting MS/MS data was performed using the Maxquant search engine based on the UniProt *decapoda* database. The setting parameters were performed according to the following: cleavage enzyme, trypsin/P; missed cleavages, 2; peptide false discovery rate (FDR), < 1%; peptide mass tolerance, 15 ppm; mass tolerance for fragment ions, 0.02 Da; fragment mass tolerance, 20 mmu; and variable modifications, oxidation on methionine (Met) and acetylation on protein N-term; and fixed modifications, carbamidomethyl on cysteine (Cys).

2.7 Bioinformatics analysis

Three comparison groups were performed in this study, including DW *vs*. FS, ST *vs*. FS, and ST *vs*. DW. The fold-change (ratio < 1/1.5 or > 1.5, $P < 0.05$) of proteins was calculated and used to identify the DAPs. GO database was conducted to assign the DAPs into cellular component, molecular function, and biological process ontology by using the InterProScan tool. KEGG database using an automatic annotation server (KAAS) was applied for the pathway description of identified DAPs. KOG database was applied for the functional classification of DAPs.

3. Results and discussion

3.1 Protein quantification and identification

The quality control checks of obtained mass spectrometry data were performed by the studies of molecular weight, peptide counts and length, and sequence coverage

177 distribution of identified proteins (Fig. 1). In total, 2,677 peptides were identified
178 based on spectral analysis. Importantly, a total of 575 proteins were identified in the
179 shrimp muscle with at least one unique peptide by spectrum search analysis with FDR
180 confidence at < 1%. The molecular weight (MW) of 413 identified proteins (71.8%)
181 ranged from 10 kDa to 60 kDa and 69 proteins (12.0%) exceeded 100 kDa (Fig. 1A),
182 which appeared to be appropriate MW distributions. The obtained results were in
183 agreement with a previous study on red shrimp (*S. melantho*) (2,158 peptides and 494
184 proteins) reported by Shi, Zhang, Lei, Shen, Yu, & Luo (2018). The distributions of
185 the obtained protein MWs were in agreement to the enzymolysis properties of trypsin
186 digestion. Most proteins (485, 84.3%) were identified by 1–10 peptides, the average
187 value being calculated as 7.0 peptides (Fig. 1B). The peptide lengths were found from
188 6 to 20 amino acids, and 90% detected peptides revealed a number of amino acids
189 lower than 22 (Fig. 1C), which conformed to the characteristics of trypsin digestion.
190 Generated peptides with less than 5 amino acids or composed of more than 20 amino
191 acids (due to their high MWs and electrical charge) were not effectively detected by
192 the MS/MS spectra. Additionally, the detected proteins were found with good
193 sequence coverage (Fig. 1D). There were 145 proteins (25.2%) with a sequence
194 coverage higher than 25% and 315 proteins (54.8%) with more than 10% sequence
195 coverage distributions of the identified proteins, which validated the feasibility and
196 availability of the experimental approaches performed during the trypsin digestion
197 and HPLC-MS/MS quantification; such analyses were found suitable for the
198 bioinformatics analyses (Chu et al., 2019).

3.2 Comparison of DAPs

The differentiation in the proteome of the three treated samples were investigated by using label-free MS/MS in order to explore the degradation of proteins in frozen shrimp after frozen storage (these words could be eliminated). From the DAP results (Table S1-S3), 224 DAPs including 61 up-regulated and 163 down-regulated were detected in DW *vs.* FS and 261 DAPs were detected in ST *vs.* DW (including 181 up-regulated and 80 down-regulated), respectively; such data were determined using a quantitative of <1/1.5 or > 1.5 and $P < 0.05$ (need to complete this sentence ?). Compared with FS samples, the large numbers of DAPs found in DW and FS suggested that significant changes occurred in shrimp muscle proteins after the frozen storage. In case of DW *vs.* FS, 112 DAPs, except for the uncharacterized proteins (Table S1), were down-regulated. These proteins included 40S ribosomal proteins (F8TCS5 and A0A0P4WSN1), actins (A1KZ91 and O96658), myosin fragment (F8QXK4), myosin heavy and light chains (A0A288ZBA6 and D4P8F7), skeletal muscle actins (A0A2H4V3E4, A0A2H4V3E2, A0A2H4V3E1, and A0A2H4V3U1), arginine kinase (P51545), Ca-transporting ATPase (U5HSJ7), L-lactate dehydrogenase (I1VSB4), paramyosin fragment (D7F2L7), ribosomal proteins (M4M7B8 and Q2I3E8), troponin C and T (A0A2P0NDU8 and A0A2P0NDU9), tropomyosin (A1KYZ2), and sarcoplasmic Ca-binding protein (C7A639), among others. These down-regulated DAPs found in DW were likely related to the destruction and/or degradation of the conformational structure of muscle proteins, mainly caused by the growth and recrystallization of ice crystals in muscle tissues

during storage. These proteomic results were in accordance with the findings of previous studies (Ma, Zhang, Deng, & Xie, 2015; Zhang, Wu, Yang, Xiang, Li, & Deng, 2017). Additionally, 41 up-regulated proteins (Table S2), except for the uncharacterized proteins, were detected in DW. These proteins included arginine kinase (Q004B5), carbonic anhydrase I (A9XTM5), citrate synthase (A0A0P4WHU5), farnesoic acid O-methyltransferase (M4QEH0), flightless-I (S4VUL7), protein disulfide-isomerase (C0JBY4), and malate dehydrogenase (A0A140AZ37). The results from DW *vs.* FS exhibited significant DAP variations, confirming the considerable changes in the proteomic trends in DW shrimp proteins after frozen storage.

Compared to DW, 261 DAPs including 181 up-regulated and 80 down-regulated were detected in ST. Except for uncharacterized proteins, the up-regulated DAPs detected in ST *vs.* DW are presented in Table S3. The proteins include 40S ribosomal proteins (G8BLI9, A0A1B2JLU1, F8TCS5, and C6EMZ8), actins (Q6DTY3 and A0T2V0), alpha-actinin (sarcomeric-like isoform x1; A0A2P1JJ58), fast-type skeletal muscle actins (A0A2H4V3E4 and A0A2H4V3E2), histones (A0A0D6DQG1 and A0A0N7G737), myosin heavy chains (Q45TX9, N0DTS3, and F8WR04), ribosomal proteins (M4M7B8, C4PL18, C4PL19, and C7SQT0), sarcoplasmic calcium-binding proteins (A0A0B5JEF0 and P02636), sodium potassium-transporting ATPase subunit (F4YYJ0), troponin T (A0A2P0NDU9), and tubulin chains (Q94570 and Q94571), among others. The detected up-regulated DAPs were positively linked with the incorporation of ST into shrimp muscle, suppressing the protein degradation in ST

and reducing the physical damage caused by the growth of ice crystals. In previous studies, ST has widely been used to maintain the WHC, retard the protein denaturation, and reduce the degeneration and physical damage to myofibers (Kingwascharapong & Benjakul, 2016). In this study, the permeated ST, as a polyanion, raised the pH of muscle, enhanced the electrostatic repulsion of proteins, and increased the distance between the polypeptide chains, which mainly contributed to the improved protein stabilization against denaturation during freezing and frozen storage (Oliveira & Goncalves, 2019). Additionally, ST molecules in muscle could show many actions, e.g. buffering, protein dispersion, oxidation inhibition, and buffering properties, which provided contributions to the protein stabilizing capabilities (Thangavelu, Kerry, Tiwari, & McDonnell, 2019). Thus, it was concluded that ST clearly improved the stability of muscle proteins detected in ST-treated samples, especially for these up-regulated DAPs, which was advantageous to shrimp muscle against the cold-induced denaturation and oxidation occurred during long-term frozen storage. In addition, the DAPs detected in FS, DW, and ST (Tables S1, S2, and S3) were identified, which could support our previous results (Zhang, Hao, Cao, Tang, Zhang, & Deng, 2018) and further provide more details for the cryoprotective roles of ST in frozen muscle during storage.

3.3 GO annotation

Annotation analyses of the DAPs expressed in FS, DW, and ST were performed by using GO database, this including three categories, i.e., molecular function, cellular component, and biological process, in order to reveal the overall trends of the

protein functions in response to the frozen storage. Compared with DW *vs.* FS (Fig. 2), the classification annotations of the DAPs exhibited similar distributions and convergences in TS *vs.* DW (Fig. 3). In the case of molecular function category, the identified DAPs were located in catalytic activity (GO:0003824) and binding (GO:0005488) terms. For cellular component category, DAPs were mainly converged in the protein-containing complex (GO:0032991), organelle (GO:0043226), cell part (GO:0044464), and cell (GO:0005623) items. Moreover, the DAPs in biological process belonged to the metabolic process (GO:0008152) and cellular process (GO:0009987). Importantly, GO categories in TS *vs.* DW changed considerably, especially for the up-regulated DAPs (annotation items) in TS, suggesting that TS treatment affected the muscle (stability) functions in frozen shrimp.

3.3.1 Molecular functions

For DW *vs.* FS (Fig. 2), skeletal muscle actins (A0A2H4V3E2, A0A2H4V3E4, A0A2H4V3U1, A0A2H4V3E1, K4EG00, C1J9C3, and B6EAU4) were located in the binding ontology. These detected proteins played dominant roles in maintaining the normal organization, structure, and functioning of the muscle tissues (Poleti et al., 2018), which were down-regulated in DW *vs.* FS mainly affected by the physical damage of the formed ice crystals. Myosin heavy (including type 1, a, and b; K4Q111, F8WR03, and F8WR04) and light (D4P8F7) chain belonged to the binding ontology and (?) were found also down-regulated in DW *vs.* FS. As the main myofibrillar components in shrimp muscle, these proteins were responsible for the relaxation and contraction (physical function) of muscle fibers. During frozen storage, the physical

287 strength of the myofibrils would be reduced greatly by the large ice crystals and
288 protein aggregation that was induced by the cold-stress (Shi, Zhang, Lei, Shen, Yu, &
289 Luo, 2018). Additionally, the growth of ice crystals also damaged the connective
290 tissues in DW *vs.* FS, thus affecting the structure and function of projectin (Q86GD6;
291 down-regulated) also located in the molecular function item. Moreover, the down-
292 regulated DAP of arginine kinase (Q004B5) was also found in DW *vs.* FS, which had
293 the ability of ATP regeneration in tissues. During long period storage, the cold-stress
294 deactivated the catalytic activity of arginine kinase, thus seriously destroying the
295 energy metabolism and homeostasis in the muscle system (Shi, Zhang, Lei, Shen, Yu,
296 & Luo, 2018).

297 For ST *vs.* DW (Fig. 3), actin 2, which is a skeletal muscle actin, and arginine
298 kinase along with ATP-binding functions were up-regulated in ST *vs.* DW. This
299 finding indicated that ST clearly maintained the stability of some binding proteins and
300 retarded subsequent aggregation and/or degradation during long periods of frozen
301 storage. Additionally, heat shock proteins (E9RF70, D2DWR3, E1B2T4, and
302 A0A0E3T0V0) belonging to the ATP-binding functions were up-regulated in ST,
303 which enhanced stress tolerance and provided protection against freezing perhaps by
304 stabilizing macromolecules and increasing hydrophobic interactions in muscle tissues
305 (Nakamura, Takagi, & Shima, 2009). Moreover, ST up-regulated the cytoskeletal
306 binding proteins, including myosin heavy chains, flightless-I (S4VUL7), alpha-
307 actinin, sarcomeric-like isoform X1 (A0A2P1JJ58), myosin (fragment, F8QXK4), and
308 profilin (A5J297). Notably, some DAPs, e.g. serine/threonine-protein phosphatase

(A0A1M4BLV5) with phosphatase activities, phosphoglycerate kinase (A0A0P4WMP5) with phosphotransferase activities, and ATP-dependent 6-phosphofructokinase (A0A193CGZ5) with 6-phosphofructokinase activities were up-regulated in TS, due to the inclusion and subsequent transference of the phosphate groups.

3.3.2 *Cellular components*

Variations in cellular components and their interactions greatly affected muscle quality properties. In this study, the detected DAPs were mainly located in the protein-containing complex, cell, cell part, and organelle items. The DAPs identified in DW, compared to FS, including myosin heavy chains, troponin I (component of troponin complex), and ribosomal proteins (in ribosome organelle) were classified into the cell part and cell annotations, which were found down-regulated, presumably resulting from the freezing-induced oxidation and/or degradation caused by the activity of reactive oxygen species (ROS) (Zhang, Fang, Hao, & Zhang, 2018). These observations agreed partially with previous findings of frozen red shrimp (*S. melantho*) (Shi, Zhang, Lei, Shen, Yu, & Luo, 2018); furthermore, the detected histones (including type H3, H4, H2A, and H2B; A0A0P4WMJ1, A0A0P4VPL0, A0A0D6DQG1 and A0A0N7G737) also exhibited similar variations. In such study, histones (components of protein-DNA complex) were correlated with muscle cell reactions to the environmental stressors, including the freezing and frozen storage, hot, and oxidative stress. Additionally, the calcium-transporting ATPase (U5HSJ7), tetraspanin (A0A0P0C4Q7), and sodium/potassium-transporting ATPase subunit

alpha (A0A139Z424) were embedded in the hydrophobic region of the cell membrane and were all down-regulated in DW, indicating that the integrality and permeability of the membrane were likely destroyed by the intra- and extracellular ice crystal growth.

In ST, the main DAPs belonged to the cell and cell part annotations, especially for up-regulated proteins, compared to DW. The myosin (fragment, F8QXK4), myosin heavy chain (fragment, Q45TX9), type 4 (N0DTS3), and b (F8WR04) as components of the myosin complex in muscle were all maintained after the storage; these components are responsible for many physicochemical properties of muscle products (Liu, Puolanne, & Ertbjerg, 2014). Transmembrane proteins in the membrane, e.g. guanylate cyclase (Q24LS5), *β*-actin (fragment, Q8WQ49), sodium-calcium exchanger (A0A110A0P3), and tetraspanin, were up-regulated in ST, indicating that the stability and integrity of membrane components were improved by the incorporation of ST molecules. Similarly, some identified DAPs in the cytoplasm, including the ATP-dependent 6-phosphofructokinase (A0A193CGZ5), importin subunit alpha (A0A1X8VIL6), and polyadenylate-binding protein (A0A0P4WRL4), were affected by the ST. Additionally, the up-regulated histones in TS *vs.* DW may improve the resistance to cold stress. Profilin (A5J297) and adenylyl cyclase-associated protein (A0A2P1JJ70) (cytoskeleton proteins) were down-regulated in DW *vs.* FS and up-regulated in TS *vs.* DW. These proteins maintain the cellular shape and play important roles in other cellular functions. Overall, TS maintained the stability of myosin complexes and transmembrane proteins, as well as preserved several cytoskeleton proteins from the structural damage against the growth and/or

353 recrystallization of ice crystals in the muscle fibers (Grasmeijer, Stankovic, De Waard,
354 Frijlink, & Hinrichs, 2013).

355 ***3.3.3 Biological processes***

356 In term of biological process annotation, ribosomal protein (type L3, L8, and
357 L18; C4PL18, Q2I3E8, and M4M7B8), 60S ribosomal protein (type L18a,
358 A0A0P4WSN1), and 40S ribosomal protein (type S3a, F8TCS5) belonged to the
359 cellular process item and were found down-regulated in DW *vs.* FS. According to
360 previous literature, ribosomal proteins, as the main ribosomal components, showed
361 the preservation ability for tRNA stability in the muscle system (Fan, Wang, Miao,
362 Liao, Ye, & Lin, 2016). Shi, Zhang, Lei, Shen, Yu, & Luo (2018) reported that the
363 down-regulation of ribosomal proteins in red shrimp that occurred after frozen storage
364 was consistent with the findings of the current study. Compared to DW, these
365 ribosomal proteins were up-regulated in ST, which may be associated with cold
366 temperature resistance and showed to improve muscle protein stability. Moreover,
367 similar changes were also found in myosin heavy chains in the ST *vs.* DW and DW *vs*.
368 FS. These proteins were also involved in the microtubule-based process of shrimp
369 muscle, including the motor-driven movement along microtubules and movement
370 driven by polymerization or depolymerization of microtubules. According to the
371 biological process annotation, these identified DAPs were associated with the
372 glycolytic metabolism and/or tricarboxylic acid (TCA) cycle in shrimp muscle. The
373 common DAPs, down-regulated in DW *vs.* FS and up-regulated in TS *vs.* DW,
374 included phosphopyruvate hydratase (A0A0S1LKK8), phosphoglycerate mutase

(A0A0P4WYI4), phosphoglycerate kinase (A0A0P4WMP5), malate dehydrogenase (A0A0P4WLG3), and glyceraldehyde-3-phosphate dehydrogenase (A0A2S1P7N3). Interestingly, malate dehydrogenase and glyceraldehyde-3-phosphate dehydrogenase were found abundantly in muscle showed a positive relationship with the color stability of muscle products (Gao, Wu, Ma, Li, & Dai, 2016; Schilling, et al., 2017). The previous literature also suggested that phosphoglycerate mutase was closely associated with the muscle quality (Mekchay, Teltathum, Nakasathien, & Pongpaichan, 2010). Thus, the stability of the muscle color during storage was improved by the incorporated ST simultaneously and was likely connected with regulated DAPs in shrimp muscle. Moreover, the GO annotation and DAP identification results in the current study were also consistent with the previous findings by Kingwascharapong & Benjakul (2016).

3.4 KEGG pathway analysis

KEGG pathway analysis was carried out to understand the biological functions, reaction networks, and the specific pathways related to DAPs, which led to different muscle quality traits. Top 20 KEGG pathways in DW *vs.* FS and TS *vs.* DW are presented in Figs. 4 and 5, respectively. In DW *vs.* FS, the significant interactions were related to the ribosome (ko03010), phagosome (ko04145), phototransduction (ko04745), hippo signaling pathway (ko04391), carbon metabolism (ko01200), and metabolic pathways (ko01100). There were 14 up-regulated and 27 down-regulated DAPs associated to metabolic pathways detected in DW, compared with FS, specifically including phosphopyruvate hydratase, phosphoglycerate mutase,

phosphoglycerate kinase, malate dehydrogenase, L-lactate dehydrogenase, ATP synthase subunit, and arginine kinase, among others. Moreover, the metabolic pathways, coupled with carbon metabolism, glycolysis, oxidative phosphorylation, and TCA cycle, were also observed in frozen muscle tissues, which were likely connected with the meat quality during freezing and subsequent frozen (?) storage (He, Huang, Li, & Yang, 2018). These results indicated that the metabolic pathway and its coupled signaling systems were of great importance to the quality variations of frozen muscle during a long-period storage. Moreover, the ribosome pathway was involved with the ribosomal proteins (type L3, L8, and L18), 60S ribosomal proteins (type L7a and L18a), and 40S ribosomal protein S3a, among others, which might be associated with the degradation of proteins and the changes of muscle traits (Liu, Men, Chang, Feng, & Yuan, 2017).

After frozen storage, samples corresponding to DW condition exhibited obvious changes in KEGG pathways, while ST treatment up-regulated the metabolic, phagosome, ribosome, carbon metabolism, protein processing in endoplasmic reticulum, and phototransduction pathways considerably compared to DW treatment. For the metabolic and carbon metabolism pathways, the up-regulated DAPs in ST included ATP synthase subunit, malate dehydrogenase, arginine kinase, glyceraldehyde-3-phosphate dehydrogenase, malate dehydrogenase, and phosphoglycerate mutase, among others. Most of these DAPs were involved in the transformation and/or modification of anionic phosphate groups on the proteins, which were mainly affected by the increased amount of phosphorus elements found in

muscle tissues. The up-regulated phagosome, hippo signaling, and phototransduction pathways influenced by ST treatment were related to DAPs, including actin, skeletal muscle actins (type 8, 9, 15, and 18), *β*-actin (fragment), tubulin alpha chain, and specific actin 1. It is likely that ST maintained the stability of these DAPs and protected them from degradation during frozen storage, thus resulting into KEGG pathway changes. Additionally, variations in the ribosome pathway were connected with the expression of ribosomal proteins, including 40S ribosomal protein types S12, S30, S3a, and SA, ribosomal protein types 8, L3, L7, L19, and P1, and ribosome-like protein. Thus, it was concluded that ST treatment affected the abundance of ribosomal proteins and subsequently regulated the ribosome pathway. Collectively, these findings suggested that TS treatment may positively affect the maintenance of muscle protein stability by affecting metabolic, ribosome, and carbon metabolism pathways, among others.

3.5 KOG analysis

The KOG function classifications of the DAPs in DW *vs.* FS and ST *vs*. DW were divided into 23 functional categories (Fig. 6). Based on the results, the top 5 functional categories in both comparisons included the “cytoskeleton”, “posttranslational modification, protein turnover and chaperones”, “signal transduction mechanisms”, “translation, ribosomal structure and biogenesis”, and “energy production and conversion”. The DW *vs.* FS and ST *vs.* DW results exhibited similar KOG distributions and changes, which indicated that there were similar variations in the proteomics analysis in DW *vs.* ST after frozen storage. Importantly,

441 the cytoskeleton function played an important role in muscle protein variations and
442 was mainly involved with the myosin regulatory light chain (KOG0031), Ca^{2+}-
443 binding actin-bundling protein (KOG0035), myosin class II heavy chain (KOG0161),
444 actin-binding cytoskeleton protein (KOG0518), actin and related proteins
445 (KOG0676), α- and β-tubulin (KOG1376 and KOG1375), troponin (KOG3634), and
446 tropomodulin and leiomodulin (KOG3735). In frozen muscle, formation of ice
447 crystals increased continuously, and their number was prone to be minimized, while
448 the distribution, orientation, particle size, and shape changed in muscle tissues during
449 frozen storage. These variations induced the subsequent aggregation, cross-linking,
450 rearrangement, and irreversible denaturation of muscle proteins, thus leading to
451 ruptured myofibrils and destroyed structures (Fernández, Otero, Martino, Molina-
452 García, & Sanz, 2008). Clearly, the cytoskeleton function of muscle proteins was
453 extremely affected by freezing-induced changes during long periods of storage.
454

455 **4. Conclusion**

456 In this study, the label free-based proteomics strategy was performed to explore
457 the proteins changes in shrimp muscle, pre-soaked in DW and ST, after frozen storage
458 and was compared to FS samples. Several DAPs were significantly detected in DW
459 *vs.* FS, which indicated that great variations occurred in muscle proteins after 30 days
460 of frozen storage, mainly induced by the cold stress. Bioinformatic analyses revealed
461 that the detected DAPs in DW *vs*. FS were connected with the metabolic, cellular
462 process, catalytic activity, and binding GO categories, which were mainly located in

the ribosome, carbon metabolism, phagosome, and metabolic KEGG pathways. Interestingly, the ST soaking treatment maintained the stability of special DAPs detected in frozen shrimp muscle, which were mainly involved in the cytoskeleton KOG functions. Current findings provide proteomic insights into the stability of muscle proteins that occur in frozen shrimp pre-soaked with phosphate and are useful for future understanding of the potential cryoprotective mechanisms.

Acknowledgments This study was funded by the National Natural Science Foundation of China (No. 31871871) and the Zhejiang Natural Science Foundation of China (Grant No. LY18C200008).

References

Chu, C., Yan, N., Du, Y., Liu, X., Chu, M., Shi, J., et al. (2019). iTRAQ-based proteomic analysis reveals the accumulation of bioactive compounds in Chinese wild rice (*Zizania latifolia*) during germination. *Food Chemistry*, *289*, 635-644.

Gao, X., Wu, W., Ma, C., Li, X., & Dai, R. (2016). Postmortem changes in sarcoplasmic proteins associated with color stability in lamb muscle analyzed by proteomics. *European Food Research and Technology*, *242*, 527-535.

Grasmeijer, N., Stankovic, M., De Waard, H., Frijlink, H. W., & Hinrichs, W. L. J. (2013). Unraveling protein stabilization mechanisms: Vitrification and water replacement in a glass transition temperature controlled system. *Biochimica et Biophysica Acta*, *1834*, 763-769.

485 Fan, L., Wang, A., Miao, Y., Liao, S., Ye, C., & Lin, Q. (2016). Comparative
486 proteomic identification of the hepatopancreas response to cold stress in white
487 shrimp, *Litopenaeus vannamei*. *Aquaculture*, *454*, 27-34.
488 Fernández, P. P., Otero, L., Martino, M. M., Molina-García, A. D., & Sanz, P. D.
489 (2008). High-pressure shift freezing: Recrystallization during storage. *European*
490 *Food Research & Technology*, *227*, 1367-1377.
491 He, Y., Huang, H., Li, L. H., & Yang, X. (2018). Label-free proteomics of tilapia
492 fillets and their relationship with meat texture during post-mortem storage. *Food*
493 *Analytical Methods*, *11*, 3023-3033.
494 Kingwascharapong, P., & Benjakul, S. (2016). Effect of phosphate and bicarbonate
495 replacers on quality changes of raw and cooked pacific white shrimp as
496 influenced by the repeated freeze-thawing. *International Journal of*
497 *Refrigeration*, *67*, 345-354.
498 Liu, J., Men, J., Chang, M., Feng, C., & Yuan, L. (2017). iTRAQ-based quantitative
499 proteome revealed metabolic changes of *Flammulina velutipes* mycelia in
500 response to cold stress. *Journal of Proteomics*, *156*, 75-84.
501 Liu, J., Puolanne, E., & Ertbjerg, P. (2014). Temperature induced denaturation of
502 myosin: Evidence of structural alterations of myosin subfragment-1. *Meat*
503 *Science*, *98*, 124-128.
504 Mekchay, S., Teltathum, T., Nakasathien, S., & Pongpaichan, P. (2010). Proteomic
505 analysis of tenderness trait in Thai native and commercial broiler chicken
506 muscles. *The Journal of Poultry Science*, *47*, 8-12.

507 Nakamura, T., Takagi, H., & Shima, J. (2009). Effects of ice-seeding temperature and
508 intracellular trehalose contents on survival of frozen *Saccharomyces cerevisiae*
509 cells. *Cryobiology*, *58*, 170-174.
510 Ocaño-Higuera, V. M., Maeda-Martínez, A. N., Marquez-Ríos, E., Canizales-
511 Rodríguez, D. F., Castillo-Yáñez, F. J., Ruíz-Bustos, E., et al. (2011). Freshness
512 assessment of ray fish stored in ice by biochemical, chemical and physical
513 methods. *Food Chemistry*, *125*, 49-54.
514 Oliveira, M. E., & Goncalves, A. A. (2019). The effect of different food grade
515 additives on the quality of Pacific white shrimp (*Litopenaeus vannamei*) after
516 two freeze-thaw cycles. *LWT-Food Science and Technology*, *113*, 108301.
517 Poleti, M. D., Moncau, C. T., Silvavignato, B., Rosa, A. F., Lobo, A. R., Cataldi, T. R.,
518 et al. (2018). Label-free quantitative proteomic analysis reveals muscle
519 contraction and metabolism proteins linked to ultimate pH in bovine skeletal
520 muscle. *Meat Science*, *145*, 209-219.
521 Schilling, M. W., Suman, S. P., Zhang, X., Nair, M. N., Desai, M. A., Cai, K., et al.
522 (2017). Proteomic approach to characterize biochemistry of meat quality defects.
523 *Meat Science*, *132*, 131-138.
524 Shi, J., Lei, Y., Shen, H., Hong, H., Yu, X., Zhu, B., & Luo, Y. (2019). Effect of
525 glazing and rosemary (*Rosmarinus officinalis*) extract on preservation of mud
526 shrimp (*Solenocera melantho*) during frozen storage, *Food Chemistry*, *272*, 604-
527 612.
528 Shi, J., Zhang, L., Lei, Y., Shen, H., Yu, X., & Luo, Y. (2018). Differential proteomic

529 analysis to identify proteins associated with quality traits of frozen mud shrimp
530 (*Solenocera melantho*) using an iTRAQ-based strategy. *Food Chemistry*, *251*,
531 25-32.
532 Thangavelu, K. P., Kerry, J. P., Tiwari, B. K., & McDonnell, C. K. (2019) .Novel
533 processing technologies and ingredient strategies for the reduction of phosphate
534 additives in processed meat. *Trends in Food Science & Technology*, *94*, 43-53
535 Wachirasiri, K., Wanlapa, S., Uttapap, D., & Rungsardthong, V. (2016). Use of amino
536 acids as a phosphate alternative and their effects on quality of frozen white
537 shrimps (*Penaeus vanamei*). *LWT-Food Science and Technology*, *69*, 303-311.
538 Wang, L., Li, J., & Zhang, L. (2015). Determination of polyphosphates in fish and
539 shrimp muscles by capillary electrophoresis with indirect UV detection after
540 phosphatase inhibition using high pressure pretreatment. *Food Chemistry*, *185*,
541 349-354.
542 Zhang, B., Cao, H. J., Lin, H. M., Deng, S. G., & Wu, H. (2019). Insights into ice-
543 growth inhibition by trehalose and alginate oligosaccharides in peeled Pacific
544 white shrimp (*Litopenaeus vannamei*) during frozen storage. *Food Chemistry*,
545 *278*, 482-490.
546 Zhang, B., Fang, C. D., Hao, G. J., & Zhang, Y. Y. (2018). Effect of kappa-
547 carrageenan oligosaccharides on myofibrillar protein oxidation in peeled shrimp
548 (*Litopenaeus vannamei*) during long-term frozen storage. *Food Chemistry*, *245*,
549 254-261.
550 Zhang, B., Hao, G. J., Cao, H. J., Tang, H., Zhang, Y. Y., & Deng, S. G. (2018). The

cryoprotectant effect of xylooligosaccharides on denaturation of peeled shrimp (*Litopenaeus vannamei*) protein during frozen storage. *Food Hydrocolloids*, *77*, 228-237.

Zhang, B., Zhao, J. L., Chen, S. J., Zhang, X. L., & Wei, W. Y. (2019). Influence of trehalose and alginate oligosaccharides on ice crystal growth and recrystallization in whiteleg shrimp (*Litopenaeus vannamei*) during frozen storage with temperature fluctuations. *International Journal of Refrigeration*. *99*, 176-185.

Zhang, B., Yao, H., Qi, H., & Ying, X. G. (2020). Cryoprotective characteristics of different sugar alcohols on peeled Pacific white shrimp (*Litopenaeus vannamei*) during frozen storage and their possible mechanisms of action. *International Journal of Food Properties*, 23(1), 95-107.

Figure captions:

Fig. 1 Molecular weight (A), peptide count (B), peptide length (C; in amino acids), and sequence coverage distribution (D) of all identified proteins in shrimp muscle.

Fig. 2 GO classifications of the DAPs identified by comparison between DW and FS batches. DAPs categorized into the biological process, cellular component, and molecular function domains.

Fig. 3 GO classifications of the DAPs identified by comparison between ST and DW batches. DAPs categorized into the biological process, cellular component, and molecular function domains.

573 Fig. 4 Top 20 KEGG pathways of the DAPs by comparison between DW and FS
574 batches.
575 Fig. 5 Top 20 KEGG pathways of the DAPs by comparison between ST and DW
576 batches.
577 Fig. 6 KOG function classifications of the DAPs by comparison between DW and FS
578 (A) and ST and DW (B) batches.
579
580 **Supplementary materials:**
581 Table S1 Down-regulated DAPs identified by label-free analysis resulting of
582 comparison between DW and FS batches.
583 Table S2 Up-regulated DAPs identified by label-free analysis resulting of comparison
584 between DW and FS batches.
585 Table S3 Up-regulated DAPs identified by label-free analysis resulting of comparison
586 between ST and DW batches

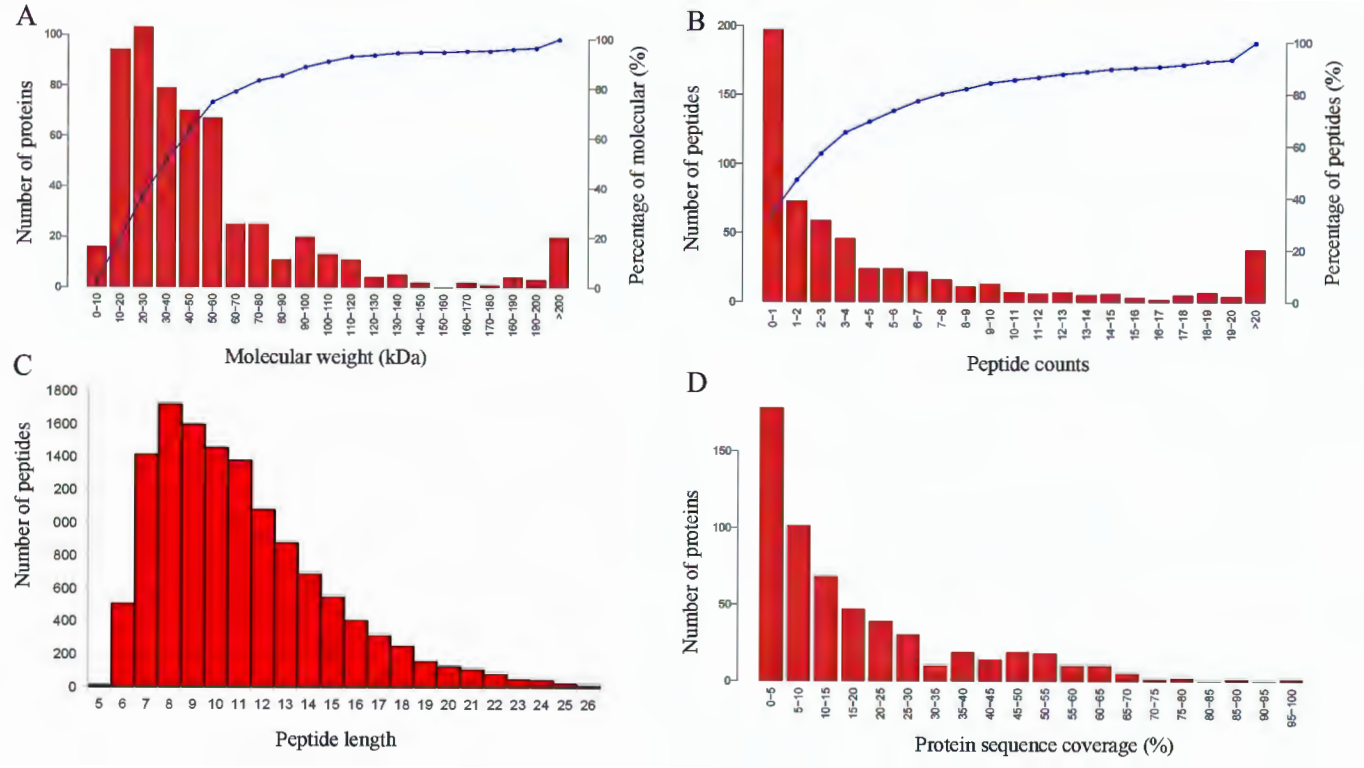
A
Number of proteins
Percentage of molecular (%)
0–10
10–20
20–30
30–40
40–50
50–60
60–70
70–80
80–90
90–100
100–110
110–120
120–130
130–140
140–150
150–160
160–170
170–180
160–190
190–200
>200
Molecular weight (kDa)
B
Number of peptides
Percentage of peptides (%)
0–1
1–2
2–3
3–4
4–5
5–6
6–7
7–8
8–9
9–10
10–11
11–12
12–13
13–14
14–15
15–16
16–17
17–18
18–19
19–20
>20
Peptide counts
C
Number of peptides
5 6 7 8 9 10 11 12 13 14 15 16 17 18 19 20 21 22 23 24 25 26
Peptide length
D
Number of proteins
0–5
5–10
10–15
15–20
20–25
25–30
30–35
35–40
40–45
45–50
50–55
55–60
60–65
65–70
70–75
75–80
80–85
85–90
90–95
95–100
Protein sequence coverage (%)

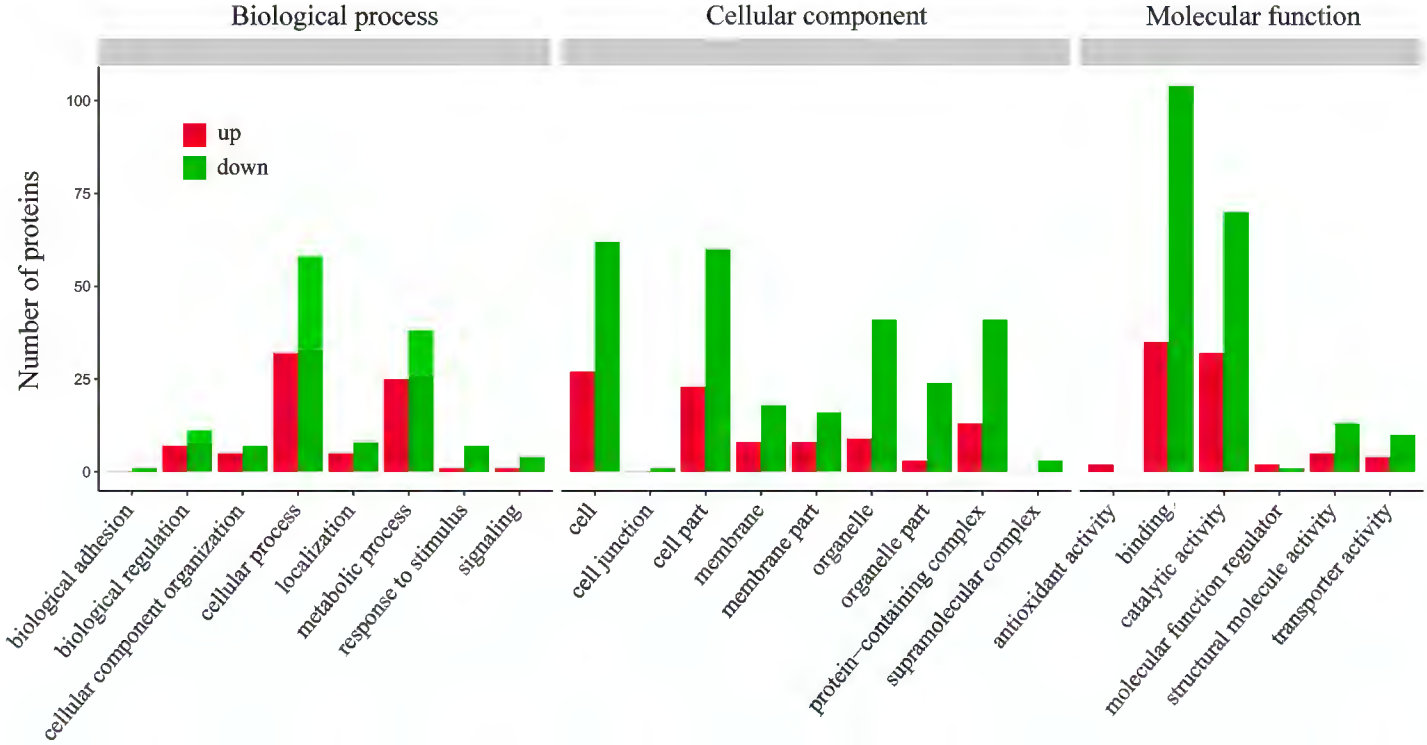
Biological process
Cellular component
Molecular function
Number of proteins
up
down
100
75
50
25
0
biological adhesion
biological regulation
cellular component organization
cellular process
localization
metabolic process
response to stimulus
signaling
cell
cell junction
cell part
membrane
membrane part
organelle
organelle part
protein−containing complex
supramolecular complex
antioxidant activity
binding
catalytic activity
molecular function regulator
structural molecule activity
transporter activity

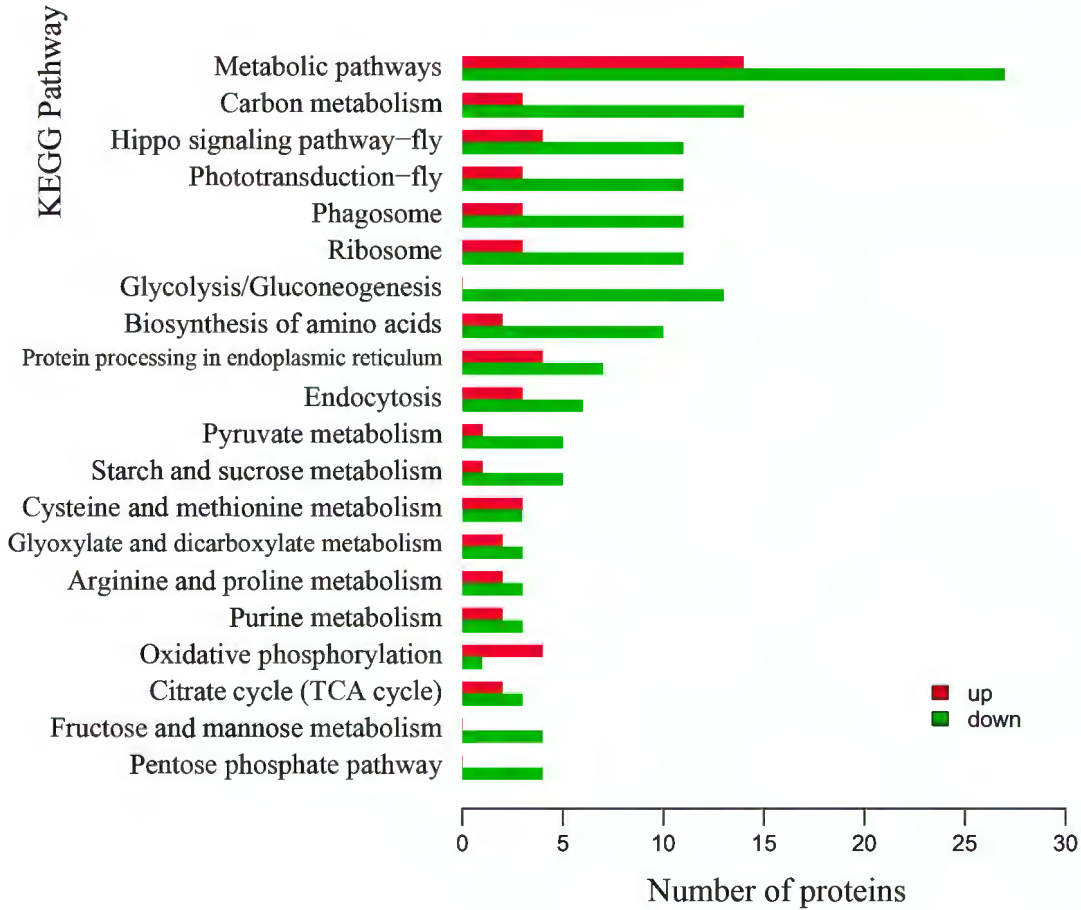
KEGG Pathway
Metabolic pathways
Carbon metabolism
Hippo signaling pathway−fly
Phototransduction−fly
Phagosome
Ribosome
Glycolysis/Gluconeogenesis
Biosynthesis of amino acids
Protein processing in endoplasmic reticulum
Endocytosis
Pyruvate metabolism
Starch and sucrose metabolism
Cysteine and methionine metabolism
Glyoxylate and dicarboxylate metabolism
Arginine and proline metabolism
Purine metabolism
Oxidative phosphorylation
Citrate cycle (TCA cycle)
Fructose and mannose metabolism
Pentose phosphate pathway
up
down
0
5
10
15
20
25
30
Number of proteins

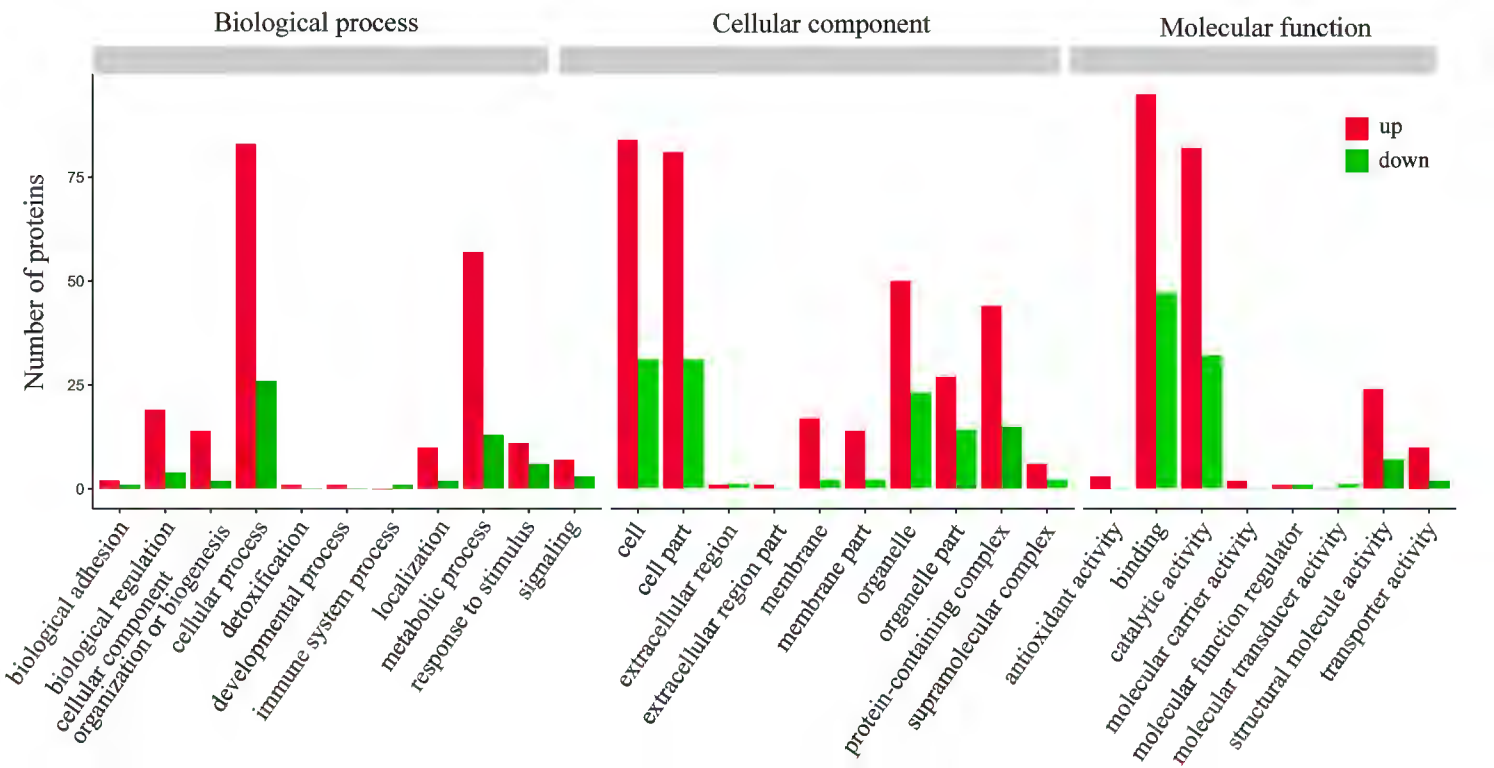
Biological process
Cellular component
Molecular function
Number of proteins
0
25
50
75
up
down
biological adhesion
biological regulation
cellular component organization or biogenesis
cellular process
detoxification
developmental process
immune system process
localization
metabolic process
response to stimulus
signaling
cell
cell part
extracellular region
extracellular region part
membrane
membrane part
organelle
organelle part
protein-containing complex
supramolecular complex
antioxidant activity
binding
catalytic activity
molecular carrier activity
molecular function regulator
molecular transducer activity
structural molecule activity
transporter activity

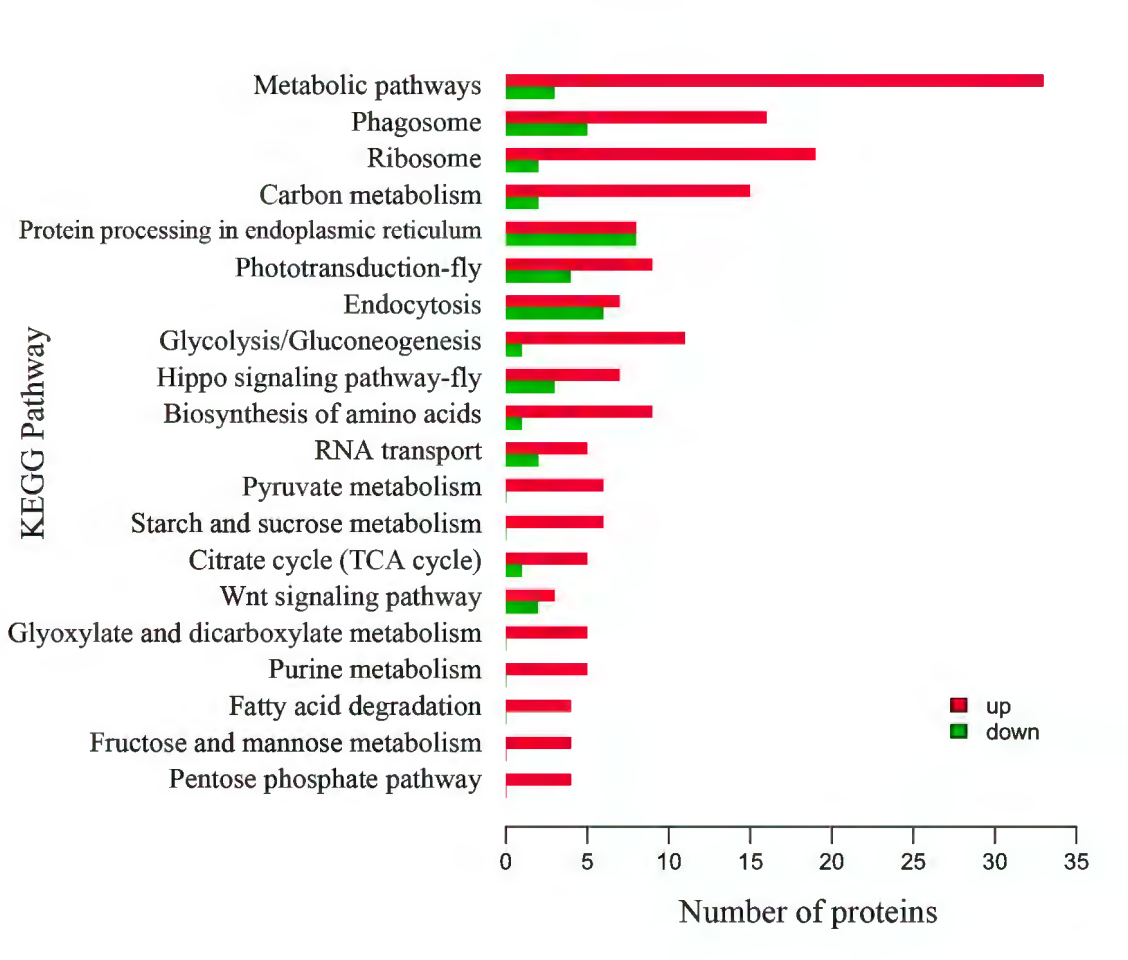
Metabolic pathways
Phagosome
Ribosome
Carbon metabolism
Protein processing in endoplasmic reticulum
Phototransduction-fly
Endocytosis
Glycolysis/Gluconeogenesis
Hippo signaling pathway-fly
Biosynthesis of amino acids
RNA transport
Pyruvate metabolism
Starch and sucrose metabolism
Citrate cycle (TCA cycle)
Wnt signaling pathway
Glyoxylate and dicarboxylate metabolism
Purine metabolism
Fatty acid degradation
Fructose and mannose metabolism
Pentose phosphate pathway
KEGG Pathway
up
down
0
5
10
15
20
25
30
35
Number of proteins

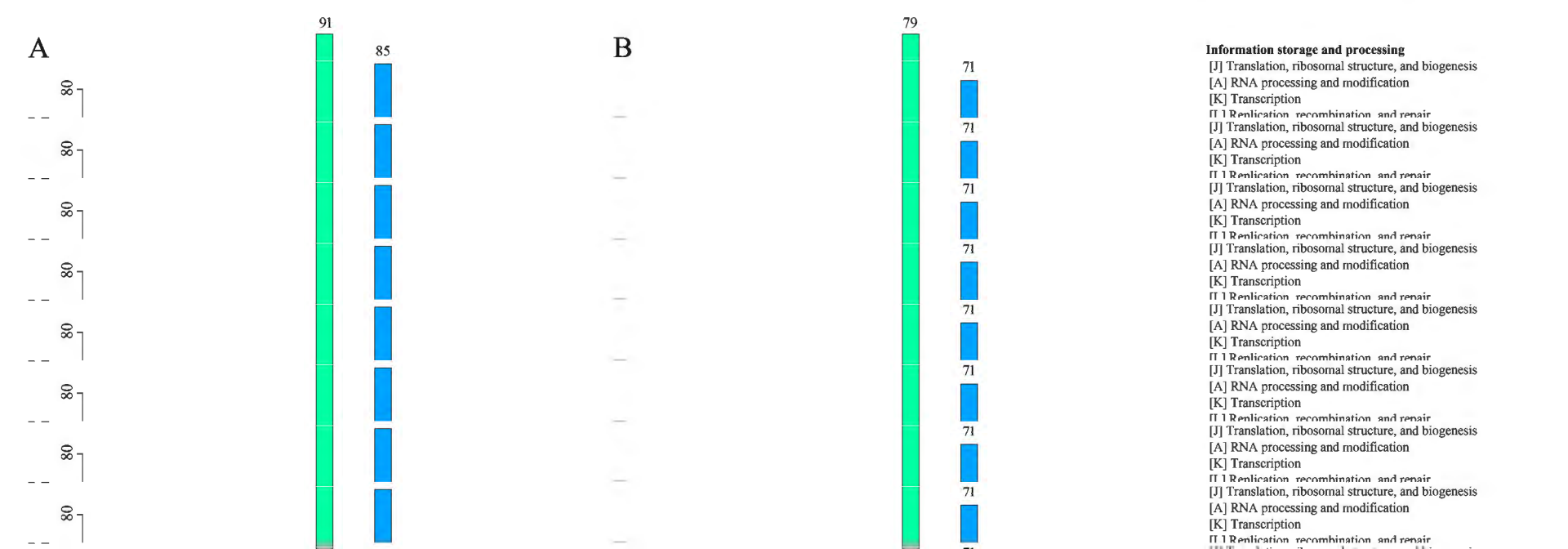
A
91
85
80
80
80
80
80
80
80
B
79
71
71
71
71
71
71
71
71
Information storage and processing
[J] Translation, ribosomal structure, and biogenesis
[A] RNA processing and modification
[K] Transcription
[J] Translation, ribosomal structure, and biogenesis
[A] RNA processing and modification
[K] Transcription
[J] Translation, ribosomal structure, and biogenesis
[A] RNA processing and modification
[K] Transcription
[J] Translation, ribosomal structure, and biogenesis
[A] RNA processing and modification
[K] Transcription
[J] Translation, ribosomal structure, and biogenesis
[A] RNA processing and modification
[K] Transcription
[J] Translation, ribosomal structure, and biogenesis
[A] RNA processing and modification
[K] Transcription
[J] Translation, ribosomal structure, and biogenesis
[A] RNA processing and modification
[K] Transcription